Comparison of recent shear capacity models with experimental and simulation databases of prestressed ultra-high-performance concrete beams

Brandon Ross, Ahmad Tarawneh, M. Z. Naser, Anca C. Ferche, Amjad Diab, and Deanna Craig

- This paper reports on an evaluation of two models for calculating the shear strength of prestressed ultra-high-performance concrete (UHPC) beams.
- Calculations from these models were compared to a database of experimental test results compiled from the literature and a simulation database developed from a machine-learning prediction model.
- The analyses show that shear strength predictions from both the models were typically conservative relative to data from the experimental and simulated databases, and both models were observed to produce less-accurate estimates for larger-sized specimens than for smaller specimens.

Compared with conventional concrete, ultra-high-performance concrete (UHPC) offers increased compressive strength, sustained postcracking resistance, and reduced vulnerability to liquid penetration. UHPC mixtures typically incorporate steel fiber reinforcement with volumetric ratios of 2% or more, and they generally have an optimized gradation of granular constituents and a water–to–cementitious materials ratio less than 0.25.[1] The first major structure to use UHPC was a pedestrian bridge built in 1997 in Quebec, QC, Canada.[1] Since that time, applications of UHPC have greatly expanded[2] and numerous research studies on UHPC have been reported.[3] In addition, design codes and standards have been developed to guide the design of UHPC structures.[4,5] UHPC has matured beyond new and novel and is now an established technology with benefits for the construction industry in general and the precast concrete industry in particular.

This paper considers the topic of shear strength in prestressed UHPC beams. Specifically, two recently introduced shear capacity models are evaluated. The first model, referred to herein as the Federal Highway Administration (FHWA) model, is described in the American Association of State Highway and Transportation Officials' draft AASHTO *Guide Specifications for Structural Design with Ultra-High Performance Concrete*.[6] Before this paper was submitted for publications, the Federal Highway Administration released a guide to assist in the design of UHPC, including shear design of prestressed sections.[7] The second model, herein referred to as the eCPCI model, comes from a research report

by Tadros et al.[8] The moniker eCPCI is based on the name of the lead company on the project (e.Construct) and the project sponsor (PCI). Although several other shear capacity models for UHPC are reported in the literature,[9] the FHWA and eCPCI models were selected for evaluation because they are of specific interest to the U.S. precast concrete industry.

The following objectives are addressed in this paper:

- Compile an experimental database of shear tests of UHPC prestressed beams.
- Compare the FHWA and eCPCI shear models against the experimental database.
- Create a machine learning model for calculating the shear strength of UHPC prestressed beams.
- Use the machine learning model to create a database of simulated shear test results (the "simulation database"). This database includes combinations of variables not found in the experimental database.
- Compare the results of the machine learning model with the eCPCI and FHWA shear capacity calculation results to further test the accuracy of the eCPCI and FHWA shear models.
- Identify gaps and shortcomings in the research on the shear strength of prestressed UHPC beams and make recommendations for future research on the topic.

UHPC overview

UHPC is attracting increased research interest, primarily because of its outstanding mechanical properties. UHPC is capable of reaching high compressive and tensile strengths, and it has excellent crack-control properties.[10,11] In addition, its durability in aggressive environments makes UHPC an attractive choice as durability and sustainability become increasingly important in design.[12,13] In some cases, the superior mechanical properties of UHPC make it possible to significantly reduce or eliminate conventional reinforcement[8,14] and allow for a higher level of prestressing and thinner sections.[15] Consequently, the use of UHPC becomes advantageous in high-performance applications such as long-span pretensioned concrete elements, bridge decks, nuclear power plant buildings, offshore platforms, elements subjected to fatigue loading, and blast- and impact-resistant structures.[16,17]

The great majority of these applications result in the UHPC material being subjected to significant shear stresses, potentially without conventional shear reinforcement provided. Consequently, an accurate determination of the shear strength of UHPC elements is paramount in the design process and for the optimal use of this material. As such, several research programs have investigated the experimental response of UHPC elements under shear loading; test variables in these programs have included UHPC mechanical properties, cross-sectional geometry, shear span–to–depth ratio, presence of prestressing, and the presence or absence of transverse reinforcement.[10,12,18–25] These experimental programs have shown that the shear response of UHPC specimens is highly influenced by the tensile behavior of UHPC. In addition, cracks in UHPC members can successfully develop as multiple and closely spaced cracks, including cases when no transverse reinforcement was provided. In an effort to understand the behavior of UHPC elements subjected to shear, Yap[25] investigated the response of UHPC membrane elements subjected to in-plane pure shear stresses. Yap concluded that the formation of multiple cracks does not appear to affect the global behavior of UHPC to the extent that it does conventional reinforced concrete. In addition, failure was characterized by crack localization that occurred before the peak shear stress. Subsequently, fibers pulled out, resulting in a gradual reduction of capacity and ductile postpeak behavior.

Tensile strength test methods and associated challenges

The tensile strength of UHPC is critical to the shear capacity of UHPC beams, especially when limited or no transverse reinforcement is provided. However, measuring the tensile strength of UHPC can be challenging, and different test methods have been used in the literature (**Fig. 1**). There is no universally accepted test method, and even the results for a single batch of UHPC can vary significantly.[26]

The experimental database compiles data derived from a variety of test methods to characterize UHPC materials. Several sources reported results of compression and tension tests, others reported only compression tests. Given the lack of consistent UHPC material testing, analyzing specimens in the database was challenging. The FHWA method (described in a subsequent section) uses three specific tensile parameters: crack localization strength $f_{t,loc}$, effective cracking strength $f_{t,cr,}$ and crack localization strain $\varepsilon_{t,loc}$. These parameters are determined through direct tension testing and are rarely reported. In the absence of direct tensile test results, the crack localization strength and the effective cracking strength were estimated for the experimental database according to the following approaches.

Method for estimating the crack localization strength

The method for estimating the crack localization strength is executed by starting with the first option and proceeding until sufficient information is available for obtaining an estimate.

1. Given $f_{t,loc}$, then $f_{t,loc} = f_{t,loc}$. If the crack localization strength is reported, it is directly used.
2. Given maximum tensile stress determined from direction tension test DT, then $f_{t,loc} \approx 0.95$DT. It is reasoned that crack localization will occur at approximately 95% of the direct tension capacity.

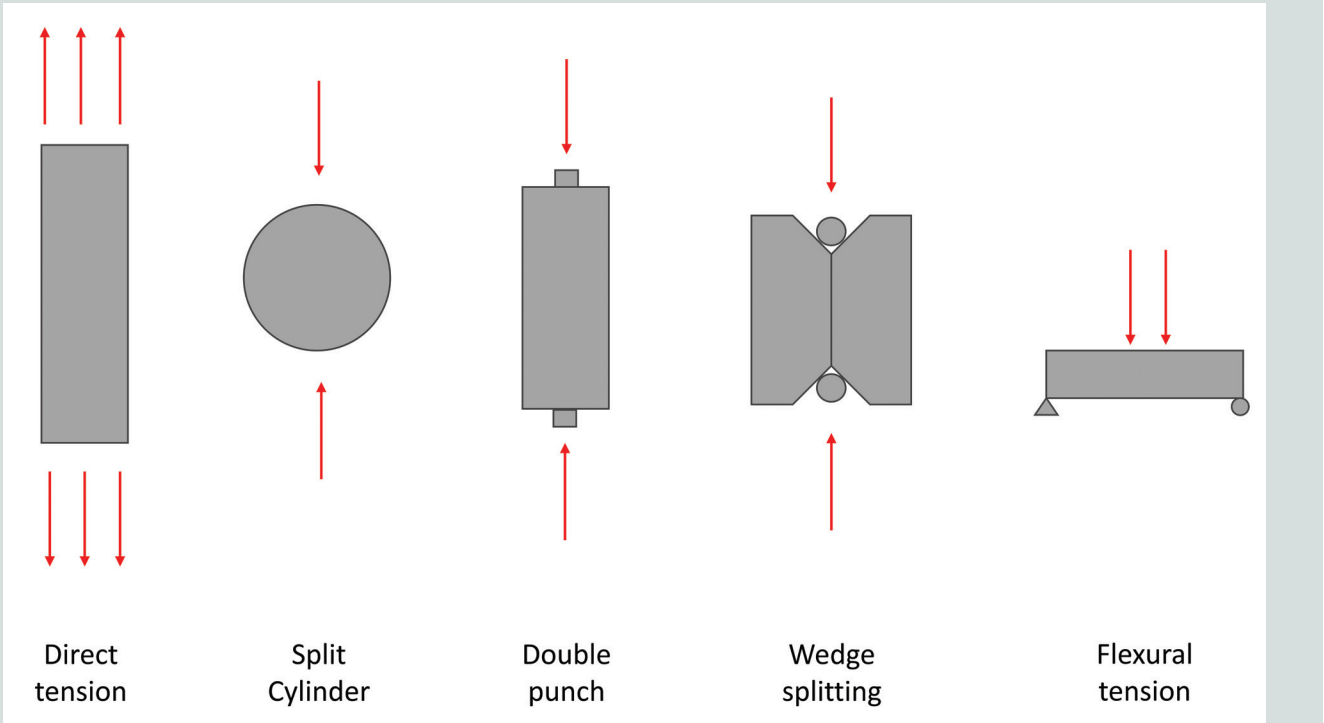

Figure 1. Methods for characterizing the tensile properties of ultra-high-performance concrete.

3. Given maximum tensile stress determined from flexural test FT, then $f_{t,loc} \approx 0.95(0.75\text{FT}) = 0.7125\text{FT}$, which is estimated based on results reported by Graybeal[12] and Voss et al.[26]

4. Given maximum tensile stress determined from split cylinder test SC, then $f_{t,loc} \approx 0.95[0.75(0.952\text{SC})] = 0.6783\text{SC}$. This estimation is based on results reported by Graybeal[12] and Voo et al.[20]

5. Given the compressive strength of UHPC f'_c, then $f_{t,loc} \approx 0.077 f'_c$. This estimation is based on results reported by El-Helou et al.[27]

The crack localization strain was taken as 0.003, which was based on the lower-bound limit of typical localization strain magnitudes compiled by El-Helou et al.[27] Given the lack of correlation among different test methods,[26] the authors acknowledge the limitation of this approach. However, in most cases in the experimental database, the data are not available for a more accurate assessment of the tensile properties required.

Approach for estimating the effective cracking strength

For this approach there are two options for estimating the cracking strength:

- If the cracking strength is reported, it is directly used as the effective cracking strength.
- If the cracking strength is not reported, it is assumed to be equal to the crack localization strength. This approach provides reasonably close estimates based on the results reported by El-Helou et al.[27]

UHPC shear models

Numerous shear capacity models have been developed over the past 20 years, and they can broadly be classified into three main groups, depending on their theoretical basis: plasticity-based models,[19,20,28–30] elasticity-based models,[31–35] and empirically-based models.[36–39] Both plasticity-based and elasticity-based models have empirical components in their formulation to account for the particularities of UHPC. In addition, in several countries, design documents were developed to incorporate specifications for the design of UHPC elements, including the International Union of Laboratories and Experts in Construction Materials, Systems, and Structures' (RILEM's) TC 162-TDF[40]; France's national standard NF P 18-47031;[41] the Swiss Society of Engineers and Architects' standard SIA 205232;[42] and design guidelines published in Germany and Spain.[43,44]

This paper focuses on two shear capacity models that are of specific interest to the precast concrete industry in the United States, namely the eCPCI model developed by Tadros et al.[8] and the FHWA model by El-Helou and Graybeal.[34] The eCPCI model was developed as part of a comprehensive research and development program that generated guidelines for the production of nonproprietary UHPC mixtures

and defined properties for a novel class of UHPC, called PCI-UHPC, suited for precast and pretensioned concrete products. Subsequently, building and bridge components using the PCI-UHPC mixtures were conceptualized, produced, and tested. Finally, design guidelines and recommendations were developed. The FHWA model proposed by El-Helou and Graybeal was developed through ongoing work by the FHWA. The FHWA method is currently being considered for inclusion in the next (10th) edition of the *AASHTO LRFD Bridge Design Specifications*.

Both models evaluate the nominal shear resistance V_n composed of the shear resistance provided by the UHPC V_{UHPC}, the shear resistance provided by conventional transverse reinforcement V_s, and the shear resistance provided by the vertical component of the effective prestressing force V_p (Eq. [1]).

$$V_n = V_{UHPC} + V_s + V_p \quad (1)$$

Both models calculate the shear resistance provided by the vertical component of the effective prestressing force V_p in accordance with the AASHTO LRFD specifications.[45] The models diverge in their evaluation of V_{UHPC} and V_s.

eCPCI model

The eCPCI shear capacity model for UHPC is based on the modified compression field theory.[46] The authors of the model[8] discourage the placement of stirrups to avoid potential fiber distribution issues; however, the eCPCI model provides a relationship for calculating the shear contribution from the transverse reinforcement for a UHPC member V_s, similar to the AASHTO LRFD specifications, assuming yielding of the transverse reinforcement. Equation (2) evaluates the shear resistance provided by UHPC V_{UHPC}.

$$V_{UHPC} = 1.33 f_{rr} b_v d_v \cot\theta \quad (2)$$

where

f_{rr} = residual tensile strength of the UHPC material = 0.75 ksi for UHPC meeting the minimum PCI-UHPC tensile requirements

b_v = effective web width taken as the minimum web width within d_v

d_v = effective shear depth

θ = angle of inclination of the diagonal compressive stress = $29 + 3500\varepsilon_s$

ε_s = net longitudinal strain at the centroid of the tension reinforcement, calculated according to the AASHTO LRFD specifications

Figure 2 provides a flowchart summarizing the eCPCI model procedure.

Equation (2) was formulated to account for the fiber and concrete contributions to the shear resistance; the term $1.33 f_{rr}$ reflects their combined influence. These contributions were derived independently. The fiber contribution is evaluated as the residual tensile strength of the UHPC material f_{rr}, which is intended to include the influence of fiber orientation, as well as size and shape effects. Tadros et al.[8] recommend that the value 0.75 ksi (5.2 MPa) be used for the residual tensile strength for UHPC meeting the minimum PCI-UHPC tensile requirements. This value was determined by applying a conversion factor of 0.375 to the specified minimum peak flexural strength of the PCI-UHPC material, 2.0 ksi (14 MPa), determined based on ASTM C1609, *Standard Test Method for Flexural Performance of Fiber-Reinforced Concrete (Using Beam with Third-Point Loading)*.[47] As such, the 0.375 factor is used to convert from the ultimate flexural strength to the postcracking tensile strength. The concrete contribution, which is intended to capture aggregate and fiber interlock, is estimated to be $0.25\cot\theta$, a value derived by following AASHTO's simplified procedure.[34] Thus, the combined fiber and concrete contribution, adjusted for the orientation of the stress field, is calculated as $(0.25 + 0.75)\cot\theta = 1.33 f_{rr}$ and the shear force resistance is derived from Eq. (2).

Last, the eCPCI model proposes a limit on the nominal shear strength using Eq. (3) intended to capture compression failure of the UHPC in the web, similar to the approach taken in AASHTO LRFD specifications[45] and CSA S6, *Canadian Highway Bridge Design Code*:[48]

$$V_n \le 0.18 f'_c b_v d_v + V_p \quad (3)$$

FHWA model

The FHWA model is based on the work of El-Helou and Graybeal,[33,34,49] as well as the principles of MCFT. Equation (4) calculates the nominal shear resistance of the UHPC material.

$$V_{UHPC} = \gamma_u f_{t,loc} b_v d_v \cot\theta \le 0.18 f'_c b_v d_v \quad (4)$$

where

γ_u = shear capacity reduction factor to account for the variability in the tensile stress in UHPC, with an upper bound of 0.85

The upper bound on V_n that captures compression failure of the UHPC within the web is given in Eq. (5).

$$V_n \le 0.25 f'_c b_v d_v + V_p \quad (5)$$

Equation (6) calculates the nominal shear resistance contribution of the transverse reinforcement V_s.

$$V_s = \frac{A_v f_{v,\alpha} d_v (\cot\theta + \cot\alpha)\sin\alpha}{s} \quad (6)$$

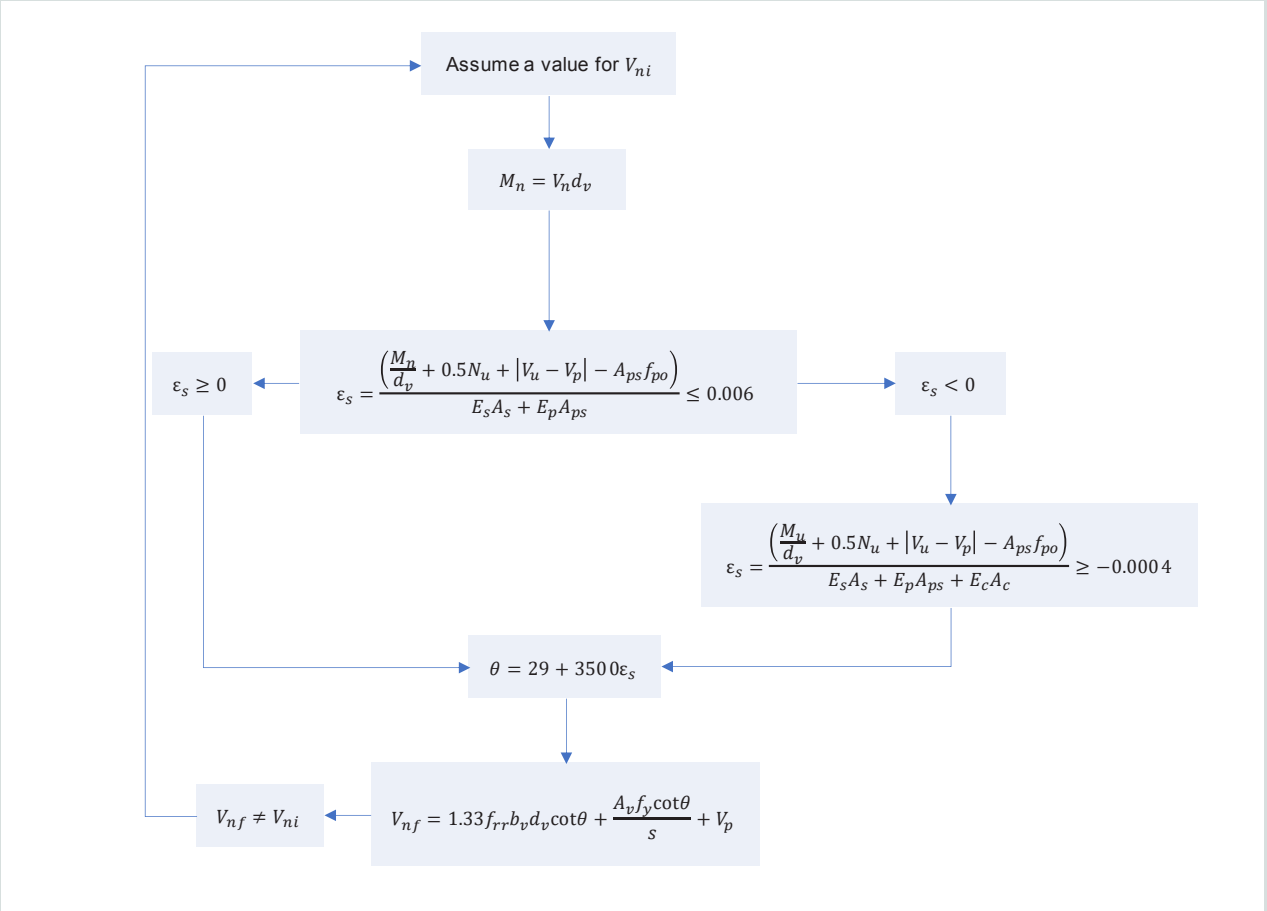

Figure 2. eCPCI shear design flowchart. Note: M_n = bending moment at the critical shear section; V_{nf} = calculated shear force at the critical shear section; V_{ni} = initial guess for the shear force at the critical shear section.

where

A_v = area of transverse reinforcement.

$f_{v,\alpha}$ = uniaxial stress in the transverse reinforcement, calculated through an iterative process with the angle θ, using Eq. (7) through (11)

α = angle of inclination of the transverse reinforcement to the longitudinal axis

s = spacing of transverse reinforcement, measured parallel to the longitudinal reinforcement

This approach removes the assumption that the transverse reinforcement is yielding when the section reaches its shear capacity, evaluating the reinforcement stress based on compatibility conditions.

$$\varepsilon_{t,loc} = \frac{\varepsilon_s}{2}\left(1+\cot^2\theta\right) + \frac{2f_{t,loc}}{E_c}\cot^4\theta + \frac{2\rho_{v,\alpha}f_{v,\alpha}}{E_c}\cot^2\theta\left(1+\cot^2\theta\right)\sin\alpha \quad (7)$$

where

ε_s = net longitudinal tensile strain in the section at the centroid of the tension reinforcement

E_c = Young's modulus of ultra-high-performance concrete

$\rho_{v,\alpha}$ = ratio of the cross-sectional area of the transverse steel reinforcement crossing the critical shear crack to the UHPC gross area along the crack projected in the longitudinal direction

$$\varepsilon_2 = \frac{2f_{t,loc}}{E_c}\cot^2\theta - \frac{2\rho_{v,\alpha}f_{v,\alpha}}{E_c}\left(1+\cot^2\theta\right)\sin\alpha \quad (8)$$

where

ε_2 = strain in the compressive strut

$$\varepsilon_v = \varepsilon_{t,loc} - 0.5\varepsilon_s + \varepsilon_2 \quad (9)$$

where

ε_v = strain along the transverse direction

$$f_{v,\alpha} = \frac{E_s \varepsilon_v}{\sin\alpha} \le f_y \quad (10)$$

where

E_s = Young's modulus of the reinforcing steel

$$\rho_{v,\alpha} = \frac{A_v}{b_v s}\left(1 + \frac{\cot\alpha}{\cot\theta}\right) \quad (11)$$

where

f_v = yield stress of transverse reinforcement

Equation (12) calculates ε_s, where $|M_u| \ge |V_u - V_p| d_v$.

$$\varepsilon_s = \frac{\left(\frac{|M_u|}{d_v} + 0.5N_u + |V_u - V_p| - A_{ps} f_{po} - \gamma_u f_{f,cr} A_{ct}\right)}{E_s A_s + E_p A_{ps}} \quad (12)$$

where

M_u = factored moment at the critical shear section

N_u = factored axial force

V_u = factored shear force at the critical shear section

f_{po} = a parameter representing prestressing level taken as modulus of elasticity of prestressing steel multiplied by the locked-in difference in strain between the prestressing steel and the surrounding UHPC

A_{ct} = area of UHPC on the flexural tension side of the member

E_p = Young's modulus of prestressing steel

A_s = area of nonprestressed steel on the flexural tension side of the member at the critical shear section

In the case where ε_s is negative or is less than the cracking tensile strain $\varepsilon_{t,cr}$, the value of ε_s is recalculated using Eq. (13).

$$\varepsilon_s = \frac{\left(\frac{|M_u|}{d_v} + 0.5N_u + |V_u - V_p| - A_{ps} f_{po}\right)}{E_s A_s + E_p A_{ps} + E_c A_{ct}} \quad (13)$$

Figure 3 illustrates the solution procedure for the FHWA model.

In the FHWA model, values for UHPC tensile properties $\varepsilon_{t,loc}$, $f_{t,loc}$, and $f_{t,cr}$ are determined through direct tension testing. Only three of the specimens in the empirical database reported data from direct tension testing, thus necessitating the approach described for estimating UHPC tensile properties (crack localization and effective cracking strength) for this study.

Machine learning and UHPC

Machine learning methods are increasingly being incorporated into structural engineering solutions, including structural health monitoring, material modeling, etc. A variety of machine learning techniques are being used to determine the mechanical and structural characteristics of concrete materials and structures. For instance, Vu and Hoang[50] developed a model using a least squares support vector machine to forecast the punching shear capability of fiber-reinforced polymer–strengthened concrete slabs. Yan and Shi[51] evaluated the potential of support vector machine in estimating the elastic modulus of both regular and high-strength concrete. In addition, Lee and Lee[52] developed a model using artificial neural network to predict the shear strength of slender fiber-reinforced concrete beams. Diab and Ferche developed an artificial neural network model to determine the tensile characteristics of UHPC based on the mix design.[53]

Another form of machine learning, by means of genetic programming, is finding its way into concrete materials and structural applications. For instance, Castelli et al.[54] successfully used genetic programming to estimate the compressive strength of high-performance concrete. Kara[55] applied genetic programming to assess the shear strength of fiber-reinforced-polymer-strengthened concrete beams without stirrups, noting superior results from the genetic programming model compared with standard design code predictions. Ahmad et al.[56] combined an artificial neural network with genetic programming to develop formulas for predicting the shear capability of steel-fiber-reinforced concrete beams lacking stirrups. To date, little work has been directed at examining the shear strength of prestressed UHPC structures.[57]

UHPC shear databases

Experimental database

To evaluate the FHWA and proposed eCPCI shear strength models, an experimental database with contributing variables was compiled. Specifically, the database includes data for 72 shear-critical prestressed UHPC beams collected from 12 studies.[8,21,27,58–66] **Table 1** provides a description of the compiled database. As provided in the references, variables surveyed for the database include cross-sectional dimensions, reported concrete properties (compression and tensile strength, elastic modulus, aggregate size), details for the steel fibers (volume and characteristics), prestressing details (area, stress, and losses), and shear reinforcement details (if any), shear span–to–depth ratio, and the experimental shear strength. **Figure 4** shows the range and distribution of some variables.

The localization tensile strength was estimated according to reported material tests and the approach elaborated on previously. The number of database beam specimens and the types of tensile strength tests used in each study include the following:

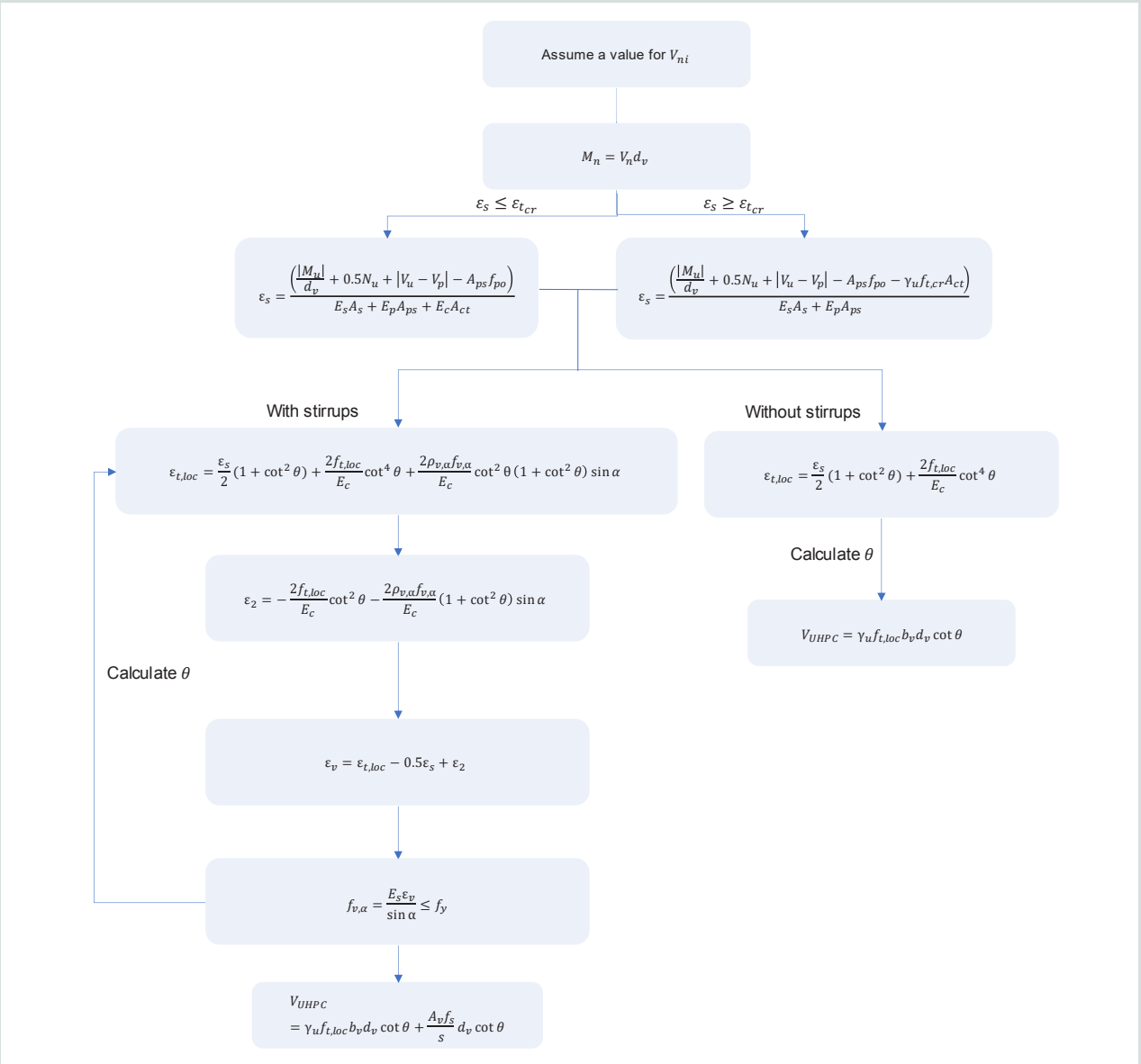

Figure 3. Federal Highway Administration shear design flowchart. Note: M_n = bending moment at the critical shear section; V_{nf} = calculated shear force at the critical shear section; V_{ni} = initial guess for the shear force at the critical shear section.

- Baby et al. (2014)[62] tested 5 beams, with UHPC tested using unnotched four-point flexural tests.
- Voo et al. (2010)[64] tested 8 beams, with UHPC tested using notched three-point flexural tests.
- Voo et al. (2006)[20] tested 6 beams, with UHPC tested using split cylinder (Brazil) or prism tensile strength, notched three-point flexural tension strength, and double punch tensile tests.
- Jin et al. (2020)[61] tested 3 beams, with UHPC tested using notched three-point flexural tests.
- Hagger and Bertram (2008)[21] tested 7 beams, with UHPC tested using flexural tension tests.
- Hegger et al. (2004)[65] tested 1 beam, with UHPC tested using flexural tension tests.
- Yang et al. (2012)[60] tested 6 beams, with UHPC tested using notched three-point flexural tension tests.
- Graybeal (2006)[66] tested 3 beams, with UHPC tested using direct tension, split cylinder (Brazil) or prism tensile strength, and four-point flexural tests.
- Zheng et al. (2019)[58] tested 8 beams, with UHPC tested using split cylinder (Brazil) or prism tensile tests.

Table 1. Database descriptions of I-shaped beams

Authors	a/d	b_v, mm	d_e, mm	ρ_{ps}, %	f'_c, MPa	ρ_f, %	ρ_v, %	V_{exp}, kN
Baby et al. (2014)	2.5	65	372	2.13	194 to 205	2.0 to 2.5	0.0 to 0.6	430 to 630
Voo et al. (2010)*	1.75 to 3.5	50	620	1.28	122 to 140	1.0 to 1.5	0	330 to 582
Voo et al. (2006)	3.3	50	600	2.66	149 to 171	1.25 to 2.5	0	330 to 497
Jin et al. (2020)	2	70	340	3.29	104 to 106	0.8	0	237 to 316
Hegger and Bertram (2008)	3.8 to 4.4	60	318	2.43 to 3.13	134 to 183	0.9 to 2.5	0	134 to 408
Hegger et al. (2004)	5.1	70	265	4.25	202	2.5	0	273
Yang et al. (2012)	2.5 to 3.4	50	640	1.9	157 to 190	1.0 to 2.0	0	437 to 717
Graybeal (2006)	2.26 to 2.83	156	808	1.6	200	2	0	1950 to 2230
Zheng et al. (2019)	1.1 to 3	50	260	4.6	111 to 113	1.6	0.6 to 1.3	249 to 368
El-Helou and Graybeal (2022)	3.06 to 3.93	76 to 102	700 to 895	2.1 to 2.3	137 to 158	2	0.0 to 3.9	1236 to 2567
Tadros et al. (2021)	1.67 to 2.79	51 to 102	776 to 1325	1.7	118 to 155	2	0.0 to 1.7	1049 to 2869
Baby et al. (2010)	2.5 to 8.5	65	305	1.5	195 to 212	1.5	0.0 to 0.6	441 to 634

* End-hooked fibers were also used in this study.

Note: a/d = shear span–to–depth ratio; b_v = effective web width taken as the minimum web width within the effective shear depth; d = distance between the extreme compression fiber of the ultra-high-performance concrete section to the resultant of the forces in the tensile reinforcement; f'_c = compressive strength of ultra-high-performance concrete; V_{exp} = experimental shear capacity results; ρ_f = fiber reinforcement ratio; ρ_{ps} = prestressed steel reinforcement ratio; ρ_v = shear reinforcement ratio. 1 mm = 0.0394 in.; 1 kN = 0.225 kip; 1 MPa = 0.145 ksi.

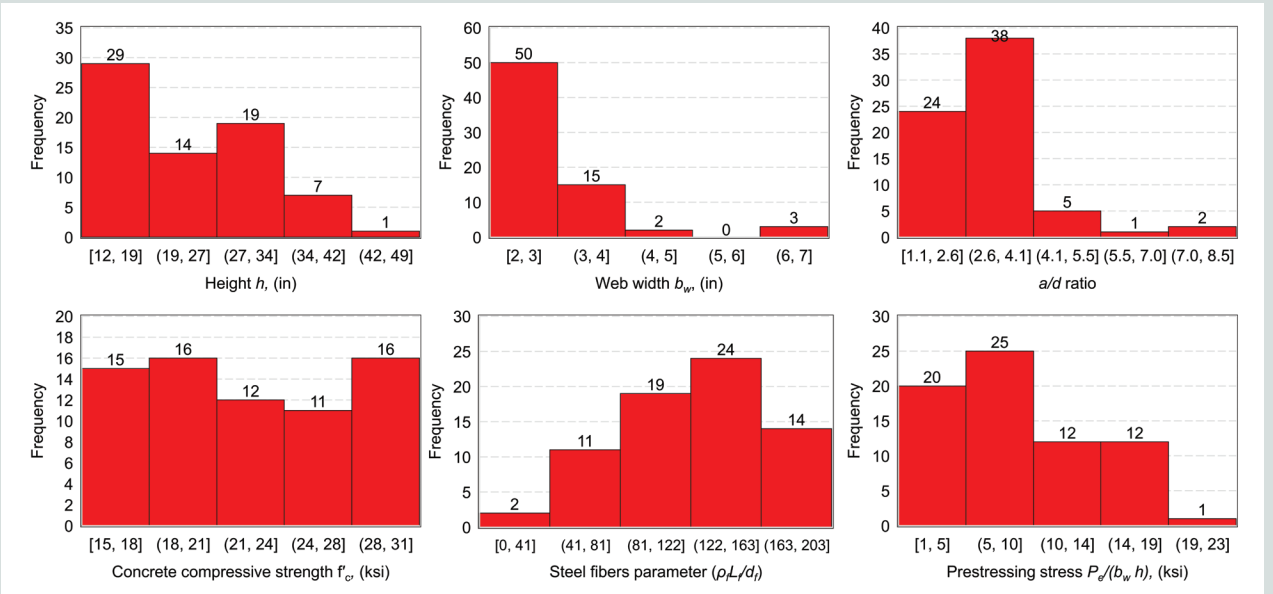

Figure 4. Range and distribution of variables in the experimental database. Note: a/d = shear span–to–depth ratio; b_w = web width; d_f = diameter of the fiber reinforcement; f'_c = compressive strength of ultra-high-performance concrete; h = total height of the beam; L_f = fiber reinforcement length; P_e = prestressing force in the critical shear section; ρ_f = fiber reinforcement ratio. 1 in. = 25.4 mm; 1 ksi = 6.895 MPa.

- Graybeal et al. (2022)[28] tested 5 beams, with UHPC tested using flexural tension tests.
- PCI UHPC report[8] tested 13 beams, with UHPC tested using flexural tension tests.
- Baby et al. (2010)[59] tested 7 beams, with UHPC tested using flexural tension tests.

In addition, straight prestressing profiles were used in all specimens, and 13 beams had shear reinforcement provided.

Simulation database

A database of 200 additional beams was created as the simulation database to expand the data available for comparing the eCPCI and FHWA models. Beams in the simulation database are hypothetical and were not physically tested. Properties of the simulated beams were uniformly distributed within the range of variables represented in the experimental database. Furthermore, practical combinations of properties were selected. For example, the transition height of the flange was coordinated with the overall beam height to ensure that the geometric dimensions of the beam were feasible and practical. The selected variables and ranges of the simulated database are provided:

- total height of the beam h = 11.8 to 35.4 in. (300 to 900 mm)
- area of UHPC on the flexural tension side of the member A_{ct} = 46.5 to 236 in.^{2} (30 × 103 to 152 × 103 mm^2)
- web width b_w = 2.0 to 5.9 in. (50 to 150 mm)
- shear span–to–depth ratio a/d = 1 to 4
- compressive strength of UHPC f'_c = 15.1 to 30.7 ksi (104 to 212 MPa)
- area of prestressing steel on the flexural tension side of the member A_{ps} = 0.3 to 10 in.^{2} (192 to 6480 mm^2)
- prestressed steel reinforcement ratio ρ_{ps} = 0 to 0.1%
- nonprestressed steel reinforcement ratio ρ_s = 0 to 0.6%
- transition depth = 0.72 to 5.3 in.^{2} (18 to 135 mm^2)
- characteristic parameter of steel fiber $\rho_f L_f/d_f$ (where ρ_f is the fiber reinforcement ratio, L_f is the fiber reinforcement length, and d_f is the diameter of the fiber reinforcement) = 21.4 to 381.9%

Artificial intelligence model for shear capacity: training, validation, and application process

This section describes how the simulated experimental capacity of the 200 beams in the simulation database was determined. **Figure 5** shows the machine learning framework used in this study. This framework has three steps: data collection, model development, and shear capacity prediction. As part of the data collection step, experimental data on UHPC beams were compiled as previously described. Several parameters were identified to govern the shear response of UHPC beams: the compressive strength of concrete f'_c, the type of steel fiber F, the characteristic parameter of steel fiber λ (which is equal to V_{fL_f}/d_f, where V_f is the fiber volume fraction), shear span a, depth d, web width b_w, tensile reinforcement ratio ρ_t, shear reinforcement ratio ρ_v, yield stress of shear reinforcement f_{ys}, and prestress level in section σ_p (which is equal to P/A_c, where P is the prestressing force and

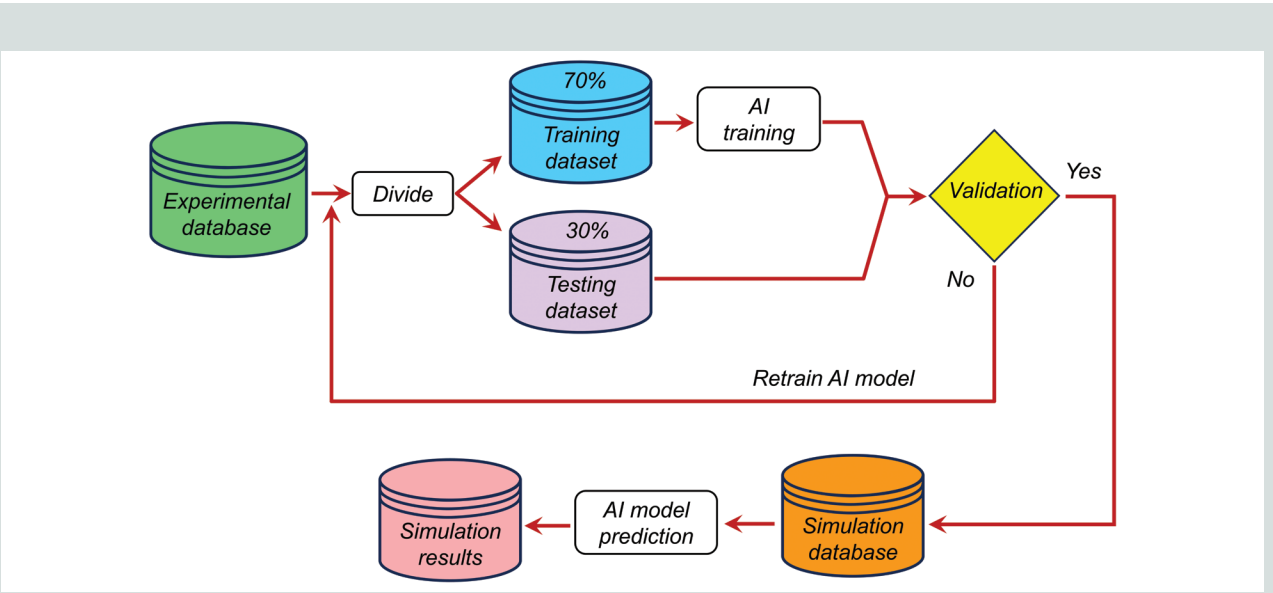

Figure 5. Machine learning model development process. Note: AI = artificial intelligence.

A_c is the area of the concrete cross section are prestressing force and area of the concrete cross section).

The simulation database is based on an extreme gradient boosting algorithm developed by Chen and Guestrin[67] as a scalable, gradient tree-based boosting model. This algorithm has been recently implemented in multiple structural engineering problems and has a tree-like structure wherein it comprises leaves that home numerical weights. Each supplied parameter (feature) to this algorithm is allocated a set of leaves that estimate an output for its sample of data. The final predicted output of the algorithm is calculated by summing the total outcome of the individual leaves. Overall, the internal structure of this algorithm is organized in such a way that minimizes the learning objective.

The objective function of the algorithm $J(\theta)$ is described in Eq. (14). This function consists of a loss component $L(\theta)$, that signifies the loss error, and a regularization term $\Omega(\theta)$.

$$J(\theta) = L(\theta) + \Omega(\theta) \tag{14}$$

The loss function in machine learning $L(\theta)$ is further expressed in Eq. (15). This function aims to arrive at accurate predictions by comparing the difference between the predicted value of the tree model $\hat{y}_i$ and the actual value of the ith sample y_i.

$$L(\Theta) = \sum_{i=1}^{n} L(y_i, \hat{y}_i) \tag{15}$$

where

n = number of predictions

Further details on the algorithm are provided by Chen and Guestrin. The algorithm was trained and validated with the experimental database. In the training and validation process, 70% of the data were used to train the model using a 10-fold cross-validation approach. In this cross-validation technique, a training set was split into 10 equal-sized subsets. In each sub-iteration, 9 subsets were used for training, and the remainder were kept for validation until all subsets were used. The other 30% of the data were used to test the model.

The performance of the machine learning model was evaluated via two metrics: the mean absolute error (Eq. [16]), and coefficient of determination R^2 (Eq. [17]).

$$\text{Mean absolute error} = \frac{\sum_{i=1}^{n} |P_i - A_i|}{n} \tag{16}$$

$$R^2 = 1 - \frac{\sum_{i=1}^{n} (P_i - A_i)^2}{\sum_{i=1}^{n} (A_i - A_{mean})^2} \tag{17}$$

where

P_i = predictions

A_i = actual measurements

A_{mean} = mean of the actual measurements

Lower values of mean absolute error and values close to positive unity for R^2 are favorable for these metrics. The selected metrics are commonly adopted and accepted in structural engineering publications.

Figure 6 shows that the machine learning model was capable of predicting the shear strength of beams in the experimental database, with R^2 being 90% in training and 89% in testing. In terms of mean absolute error, the machine learning predictions are evaluated at 32.9 and 29.4 kN (7.40 and 6.61 kip) for training and testing, respectively. Given these results, the machine learning model was then used to create the simulation database for further comparison of the eCPCI and FHWA methods.

Comparison of databases and shear models

Experimental database

Figure 7 compares the experimentally measured concrete shear strength with the calculated shear strengths from the eCPCI and FHWA models. To ensure accuracy of calculations, the authors performed calculations separately in two groups and then compared the results for consistency.

Most points with shear strength less than about 700 kN (160 kip) are scattered around a perfect fit line in Fig. 7 (the experimental shear capacity results V_{exp} equal the predicted shear capacity results V_{pred}); this observation is particularly applicable to the FHWA model. For points with a shear strength of more than about 700 kN, the data are scattered away from the perfect fit line toward the conservative side. The patterns shown in Fig. 7 are confirmed by data in **Table 2**, which presents a statistical comparison of the two models. Table 2 shows that there are 17 and 6 specimens

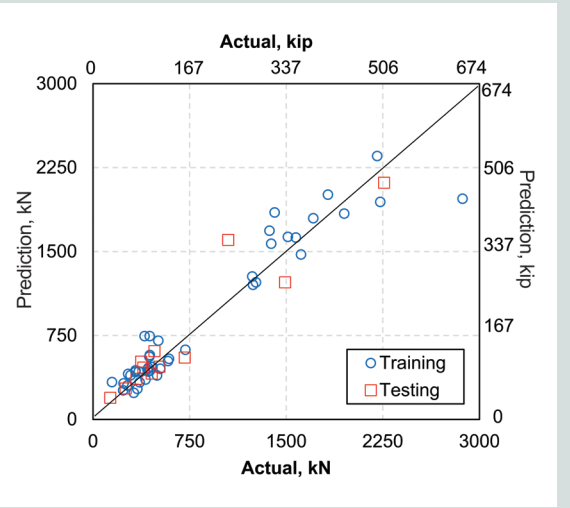

Figure 6. Training and testing of machine learning model.

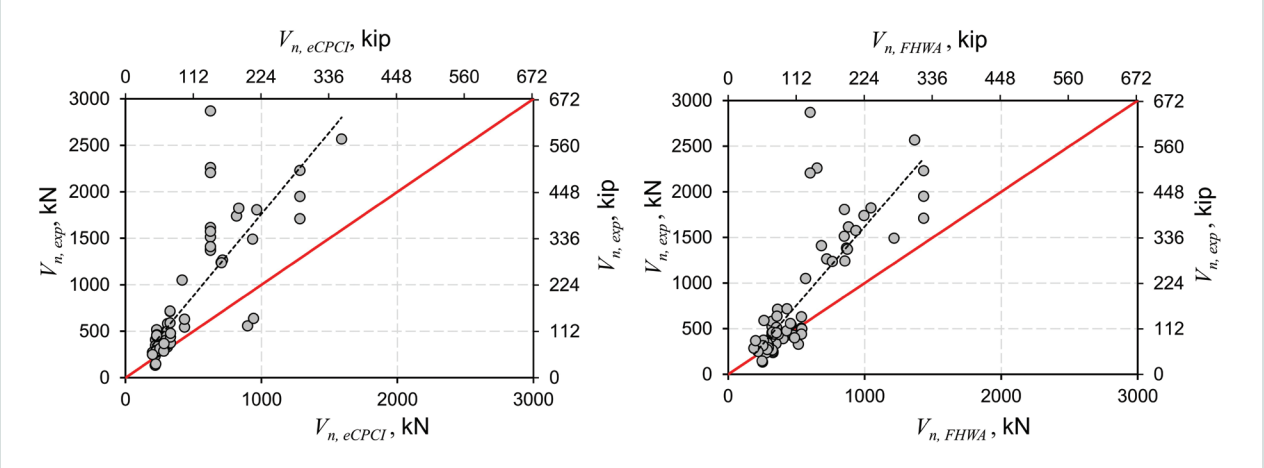

Figure 7. Experimental versus calculated shear capacities for the experimental database. Note: FHWA = Federal Highway Administration; V_{exp} = experimental shear capacity results; $V_{n,eCPCI}$ = nominal shear resistance using eCPCI method; $V_{n,FHWA}$ = nominal shear resistance using FHWA method.

with V_{exp}/V_{pred} greater than 2.0 for the eCPCI model and FHWA models, respectively. Table 2 also indicates four specimens with V_{exp}/V_{pred} less than 0.75 for both models. The eCPCI and the FHWA models resulted in average V_{exp}/V_{pred} ratios of 1.68 and 1.43, respectively, indicating higher average conservatism for the eCPCI model.

Because the results of the two models appear similar, the predictions from the two models were plotted in one graph (**Fig. 8**). Figure 8 shows that both models resulted in similar performance, with the FHWA method predicting higher shear (about 17% higher on average). The similarity of the models' predictions is also confirmed by their similar standard deviations, coefficients of variation, and root mean square errors.

For a closer look on both models, V_{exp}/V_{pred} values were plotted with respect to different variables (**Fig. 9**). A flat trendline in Fig. 9 indicates a consistent prediction conservatism across the variable range, whereas a sloped trendline indicates a change in the conservatism of the predictions.

The topmost graphs in Fig. 9 plot V_{exp}/V_{pred} with respect the concrete compressive strength and girder web width. The graphs show a relatively flat or small slope trendline, which indicates a small variation in the conservatism across the range of compressive strengths. However, when the trendline of V_{exp}/V_{pred} is examined with respect to the prestressing ratio and girder height (Fig. 9), a high positive slope is noted,

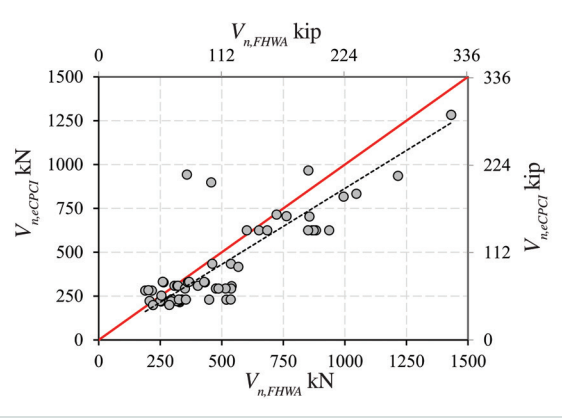

Figure 8. Comparison of calculated shear capacities from the eCPCI and Federal Highway Administration (FHWA) models. Note: $V_{n,eCPCI}$ = nominal shear resistance using eCPCI method; $V_{n,FHWA}$ = nominal shear resistance using FHWA method.

Table 2. Statistical performance of eCPCI and FHWA methods based on comparison to the experimental database using the ratio of experimental shear capacity results Vexp to predicted shear capacity results Vpred

Model	V_{exp}/V_{pred} average	V_{exp}/V_{pred} tandard deviation	V_{exp}/V_{pred} coefficient of variation, %	V_{exp}/V_{pred} root mean square error, kN	V_{exp}/V_{pred} > 2.0, number of specimens	V_{exp}/V_{pred} < 0.75, number of specimens
eCPCI	1.68	0.67	40	569	17	4
FHWA	1.43	0.67	47	521	6	4

Note: FHWA = Federal Highway Administration. 1 kip = 4.448 kN.

which indicates a significant increase in conservatism when each of the variables increases. This finding suggests that both models are less accurate (but more conservative) for larger beams.

Simulation database

Figure 10 compares the V_{exp}/V_{pred} ratios for the machine learning -stimulated results versus the eCPCI and FHWA models. Both models behaved similarly for capacities less than 1000 kN (225 kip). Beyond this range, the FHWA model predictions become unconservative. **Table 3** presents the statistical comparison of the models for the simulation database. The conclusion reached from this comparison is similar to that for the experimental database: both models have similar accuracy (on average), with slightly better predictions for the FHWA model.

Figure 11 shows the V_{exp}/V_{pred} ratios for each model with respect to different variables. In contrast to the flat-to-increasing slopes (uniform to increasing conservatism) shown in Fig. 9 for the experimental database, the slopes in Fig. 11 are flat to negative across the variables, indicating the calculation results become less conservative as the values of the input variables increase toward the higher ends of the database's range. These trends were consistent for both models. The discrepancy could be attributed to the small database used for machine learning training, but it supports the previous observation that both of the models lose accuracy for girders with larger dimensions. This finding demonstrates the need for future research to focus on larger UHPC prestressed beams. If the machine learning model has identified a real trend, the eCPCI and FHWA theoretical models become increasingly less conservative as beams become larger.

Also, the FHWA model becomes increasingly less conservative as the UHPC compressive strength increases, whereas the eCPCI conservatism is relatively consistent for all compressive strengths. The observation is consistent with the formulation of the models, wherein the eCPCI method does not consider increases in UHPC material properties, provided that they meet the associated prescriptive standards. In addition to testing larger girders, tests of girders with high UHPC strength are also recommended. While compressive strength is not directly considered in the FHWA model, tests of beams with higher UHPC strength can be used to evaluate the decreasing trend between FHWA conservatism and compressive strength.

Conclusion

This paper evaluates the prediction of shear strength for prestressed UHPC beams using the FHWA and eCPCI methodologies. The analyses used the available experimental data from the published literature on the shear strength of prestressed UHPC beams. Only a limited number of tests (70 specimens) were identified, and different test programs used different material tests to characterize the UHPC properties. Where the localized tensile strength of UHPC could not be determined from the published data, it was approximated using other tensile strength data that were reported. In addition to the empirical data in the experimental database, a machine learning prediction model was developed to generate a simulation database for further evaluation. Recommendations and conclusions from the research are provided:

- The experimental results used five different tests to characterize the UHPC tensile strength. This inconsistency in testing severely limits the ability to compare results across different research projects and assess the accuracy of UHPC shear design models. Unless the industry converges on a single material characterization test or a suite of material characterization tests, researchers should run all of the tests.

- Direct tension testing is specifically recommended for UHPC characterization in future investigations to test the shear capacity of prestressed UHPC beams. The FHWA shear capacity model uses values from direct tension tests. Shear testing programs that accompany UHPC direct tension testing will be beneficial for direct comparison with the FHWA shear model, which is advancing toward practical use by bridge designers.

- Evaluation based on the experimental database shows that both the FHWA and eCPCI methods produce similar conservative trends in estimating the shear capacity of prestressed UHPC beams, with slightly better accuracy for the FHWA method. The eCPCI and the FHWA models resulted in average V_{exp}/V_{pred} ratios of 1.68 and 1.43, respectively. The analyses showed that both models have increased conservatism for large beams.

Table 3. Statistical performance of eCPCI and FHWA methods based on comparison to the simulation database using the ratio of experimental shear capacity results V_{exp} to predicted shear capacity results V_{pred}

Model	V_{exp}/V_{pred} average	V_{exp}/V_{pred} standard deviation	V_{exp}/V_{pred} coefficient of variation	V_{exp}/V_{pred} root mean square error, kN	V_{exp}/V_{pred} > 2.0, number of specimens	V_{exp}/V_{pred} < 0.75, number of specimens
eCPCI	1.97	1.18	60%	395	69	7
FHWA	1.56	1.06	68%	398	42	33

Note: FHWA = Federal Highway Administration. 1 kip = 4.448 kN.

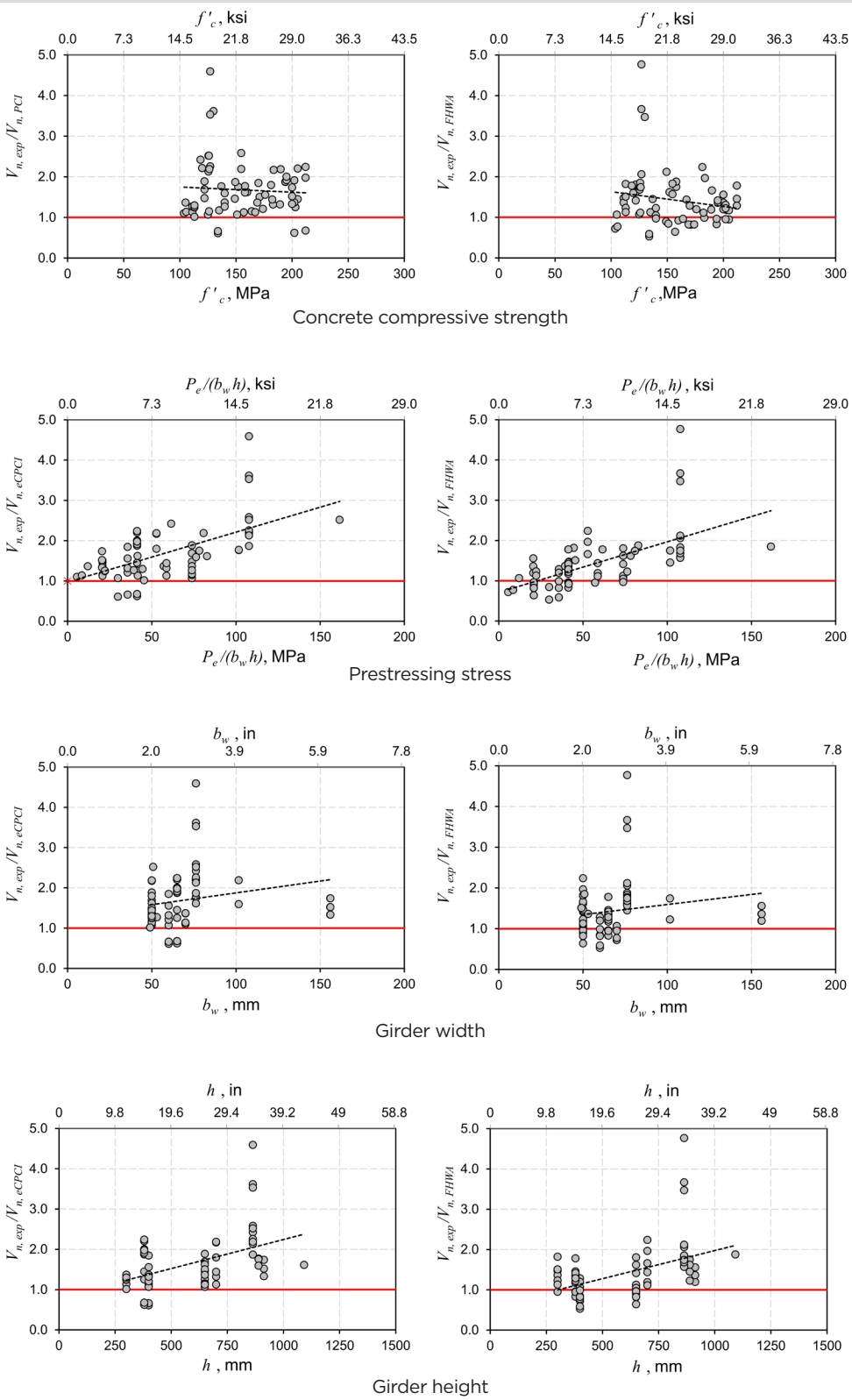

Figure 9. Ratio of experimental shear capacity results V_{exp} to predicted shear capacity results V_{pred} for eCPCI and Federal Highway Administration (FHWA) methods for the experimental database. Note: bw = web width; f'_c = compressive strength of ultra-high-performance concrete; ***h*** = total height of the beam; P_e = prestressing force in the critical shear section; $V_{n,eCPCI}$ = nominal shear resistance using eCPCI method; $V_{n,FHWA}$ = Nominal shear resistance using FHWA method.

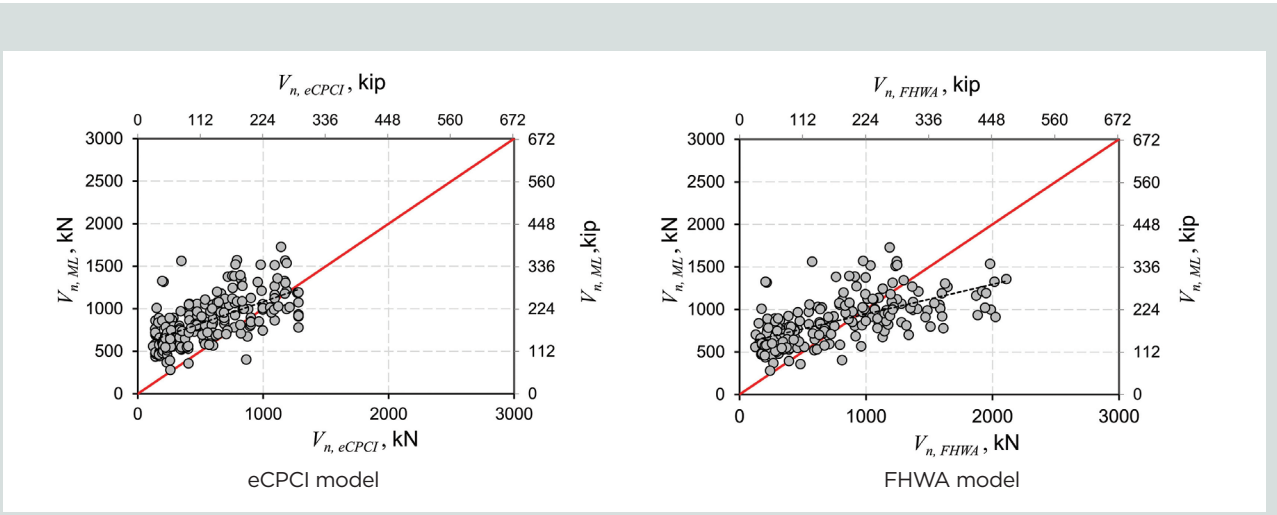

Figure 10. Experimental versus calculated shear capacities for the simulation database. Note: FHWA = Federal Highway Administration; $V_{n,eCPCI}$ = nominal shear resistance using eCPCI method; $V_{n,FHWA}$ = nominal shear resistance using FHWA method; $V_{n,ML}$ = nominal shear resistance using machine learning method.

- A comparison of the FHWA and eCPCI models against the simulation database produced comparable results in terms of similar average standards of deviation, coefficients of variation, and root mean square errors. For comparisons with the simulation database, the eCPCI and the FHWA models resulted in average V_{exp}/V_{pred} ratios of 1.97 and 1.56, respectively.

- Comparisons of both test methods and databases indicate that model accuracy decreased for specimens at the high end of the considered ranges. For the experimental database, the models were more conservative for larger beams; however, the analyses of the simulation database show a reduction in conservatism. This discrepancy may be attributed to the small database used for machine learning training. Because of the limited data, future shear testing of UHPC beams should include larger test specimens.

- The FHWA method was more accurate than the eCPCI method when compared with the databases, but the FHWA model was more difficult to implement for hand calculations due to the iterative nature of the procedure. In addition to iterations in the individual beam calculations, the research team performed multiple rounds of calculations and checking to ensure that the results converged on accurate solutions. Engineers are encouraged to use caution when calculating the shear capacity of prestressed UHPC beams using the FHWA method until familiarity and confidence with that method are developed.

Considering the limited experimental data and the assumptions made in estimating the material properties, these conclusions are considered a starting point for discussing the available design models. They should be revisited as more experimental data become available.

Acknowledgments

Funding for this research was provided by PCI through the Daniel P. Jenny Research Fellowship awarded to the University of Texas at Austin; PCI also provided funding to Clemson University in support of this research.

References

1. Blais, P. Y., and M. Couture. 1999. "Precast, Prestressed Pedestrian Bridge World's First Reactive Powder Concrete Structure." *PCI Journal* 44 (5): 60–71. https://doi.org/10.15554/PCIJ.09011999.60.71.

2. Abdal, S., W. Mansour, I. Agwa, I., M. Nasr, and Y. O. Özkılıç. 2023. "Application of Ultra-High-Performance Concrete in Bridge Engineering: Current Status, Limitations, Challenges, and Future Prospects." Buildings 13 (1): 185. https://doi.org/10.3390/buildings13010185.

3. Ullah, R., Y. Qiang, J. Ahmad, N. I. Vatin, and M. A. El-Shorbagy. 2022. "Ultra-High-Performance Concrete (UHPC): A State-of-the-Art Review." *Materials* 15 (12): 4131. https://doi.org/10.3390%2Fma15124131.

4. Bajaber, M. A., and I. Y. Hakeem. 2021. "UHPC Evolution, Development, and Utilization in Construction: A Review." Journal of Materials Research and Technology, no. 10: 1058–74. https://doi.org/10.1016/j.jmrt.2020.12.051.

5. Islam, M. M., Q. Zhang, and Q. Jin. 2022. "A Review of Existing Codes and Standards on Design Factors for UHPC Placement and Fiber Orientation." *Construction and Building Materials*, no. 345: 128308. https://doi.org/10.1016/j.conbuildmat.2022.128308.

6. Graybeal, B. A., and R. G. El-Helou. 2019. "Development of an AASHTO Guide Specification for UHPC." *Second International Interactive Symposium on UHPC* 2 (1). https://doi.org/10.21838/uhpc.9708.

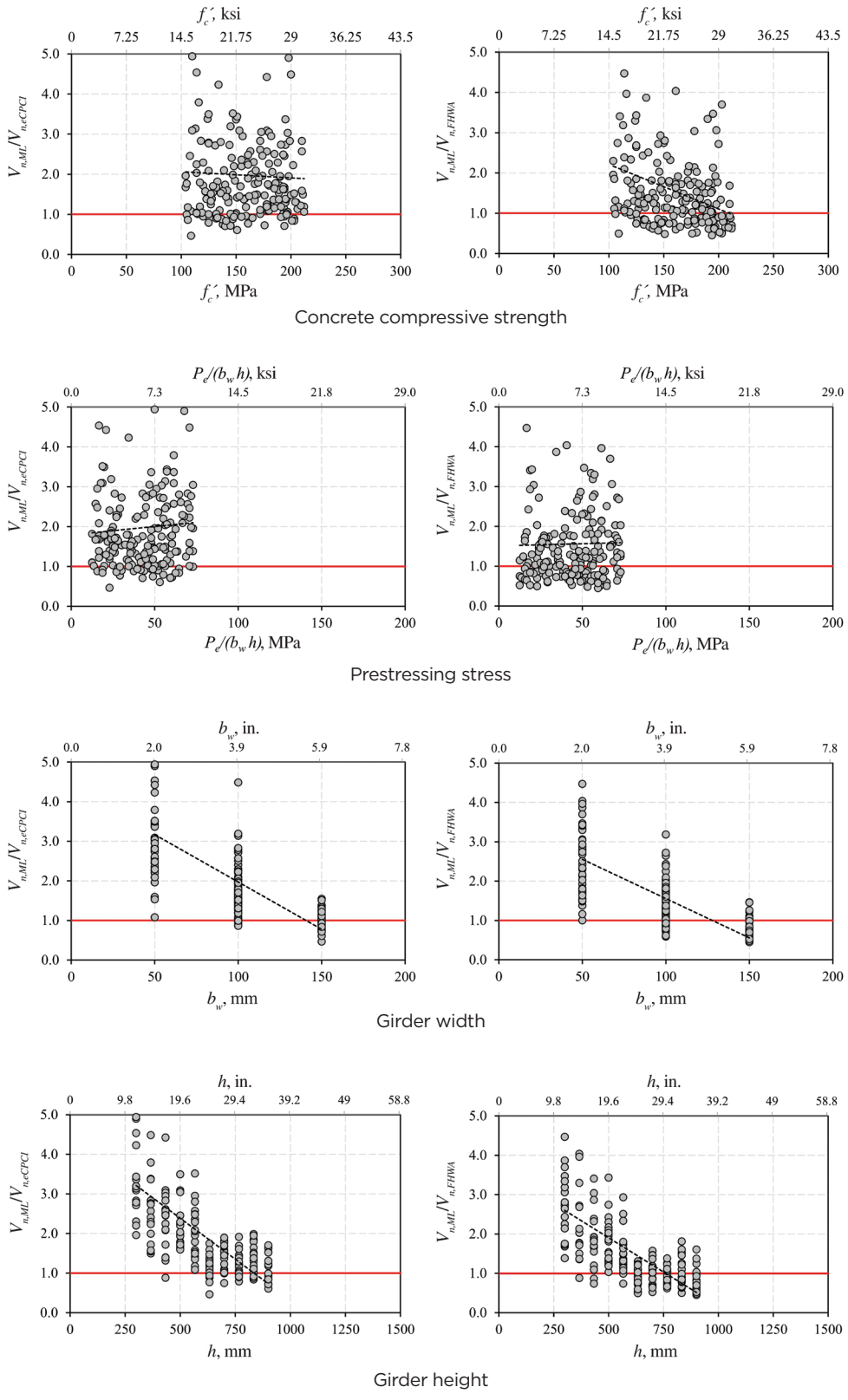

Figure 11. Ratio of machine-learning shear capacity results $V_{n,ML}$ to calculated shear capacity for results V_n for eCPCI and FHWA methods. Note: b_w = web width; f_c' = compressive strength of ultra-high-performance concrete; h = total height of the beam; P_e = prestressing force in the critical shear section; $V_{n,eCPCI}$ = nominal shear resistance using eCPCI method; $V_{n,FHWA}$ = nominal shear resistance using FHWA method; $V_{n,ML}$ = nominal shear resistance using machine learning method.

7. Graybeal, B. A., and R. G. Helou. 2023. *Structural Design with Ultra-High Performance Concrete*. FHWA-HRT-23-077. Washington, DC: FHWA (Federal Highway Administration). https://doi.org/10.21949/1521382.

8. Tadros, M., J. Lawler, M. El-Khier, et al. 2021. *Implementation of Ultra-High Performance Concrete in Long-Span Precast Pretensioned Elements for Concrete Buildings and Bridges*. Chicago, IL: PCI. https://doi.org/10.15554/pci.rr.mat-013v2.1.

9. Solhmirzaei, R., H. Salehi, V. Kodur, and M. Z. Noser. 2020. "Machine Learning Framework for Predicting Failure Mode and Shear Capacity of Ultra High Performance Concrete Beams." *Engineering Structures*, no. 224: 111221. https://doi.org/10.1016/j.engstruct.2020.111221.

10. Azmee, N. M., and N. Shafiq. 2020. "Preparation of Low Cement Ultra-High Performance Concrete." In *CIGOS 2019, Innovation for Sustainable Infrastructure: Lecture Notes in Civil Engineering*, edited by C. Ha-Minh, D. Dao, F. Benboudjema, S. Derrible, D. Huynh, and A. Tang, 331–336. Singapore: Springer. https://doi.org/10.1007/978-981-15-0802-8_50.

11. Li, J., Z. Wu, C. Shi, Q. Yuan, and Z. Zhang. 2020. "Durability of Ultra-High Performance Concrete—A Review." *Construction and Building Materials*, no. 255: 119296. https://doi.org/10.1016/j.conbuildmat.2020.119296.

12. Graybeal, B. A. 2006. *Material Property Characterization of Ultra-High Performance Concrete*. FHWA-HRT-06-103. Washington, DC: FHWA. https://rosap.ntl.bts.gov/view/dot/38714/dot_38714_DS1.pdf.

13. Kodsy, A., and G. Morcous. 2022. "Shear Strength of Ultra-High-Performance Concrete (UHPC) Beams without Transverse Reinforcement: Prediction Models and Test Data." *Materials* 15 (14): 4794. https://doi.org/10.3390/ma15144794.

14. Vítek, J. L., R. Coufal, and D. Čítek. 2013. "UHPC—Development and Testing on Structural Elements." Procedia Engineering, no. 65: 218–223. https://doi.org/10.1016/j.proeng.2013.09.033.

15. Zhou, M., W. Lu, J. Song, and G. C. Lee. 2018. "Application of Ultra-High Performance Concrete in Bridge Engineering." *Construction and Building Materials*, no. 186: 1256–1267. https://doi.org/10.1016/j.conbuildmat.2018.08.036.

16. Khan, M. U., S. Ahmad, A. A. Naqvi, and H. J. Al-Gahtani. 2020. "Shielding Performance of Heavy-Weight Ultra-High-Performance Concrete against Nuclear Radiation." *Progress in Nuclear Energy*, no. 130: 103550. https://doi.org/10.1016/j.pnucene.2020.103550.

17. Hegger, J., D. Tuchlinski, and B. Kommer. 2004. "Bond Anchorage Behavior and Shear Capacity of Ultra High Performance Concrete Beams." In *Ultra High Performance Concrete (UHPC) : Proceedings of the International Symposium on Ultra High Performance Concrete, Kassel, Germany, September 13-15, 2004*, edited by M. Schmidt, 351–360. Kassel, Germany: Kassel University Press.

18. Graybeal, B. A. 2009. *Structural Behavior of a Prototype Ultra-High Performance Concrete Pi-Girder*. FHWA-HRT-10-027. Washington, DC: FHWA. https://www.fhwa.dot.gov/publications/research/infrastructure/structures/09068/09068.pdf.

19. Voo, Y. L., S. J. Foster, and C. C. Voo. 2015. "Ultra-high-Performance Concrete Segmental Bridge Technology: Toward Sustainable Bridge Construction." *Journal of Bridge Engineering* 20 (8). https://doi.org/10.1061/(ASCE)BE.1943-5592.0000704.

20. Voo, Y. L., S. J. Foster, and R. I. Gilbert. 2006. "Shear Strength of Fiber Reinforced Reactive Powder Concrete Prestressed Girders without Stirrups." *Journal of Advanced Concrete Technology* 4 (1): 123–132. https://doi.org/10.3151/jact.4.123.

21. Hegger, J., and G. Bertram. 2008. "Shear Carrying Capacity of Ultra-High Performance Concrete Beams." In *Tailor Made Concrete Structures: New Solutions for Our Society: Proceedings of the International FIB Symposium 2008, Amsterdam, the Netherlands, 19-21 May 2008*, edited by J. C. Walraven and D. Stoelhorst, 341–347. New York: CRC Press.

22. Xia, J., K. R. Mackie, M. A. Saleem, and A. Mirmiran. 2011. "Shear Failure Analysis on Ultra-High Performance Concrete Beams Reinforced with High Strength Steel." *Engineering Structures* 33 (12): 3597–3609. https://doi.org/10.1016/j.engstruct.2011.06.023.

23. Baby, F., J. Billo, J. C. Renaud, C. Massotte, P. Marchand, and F. Toutlemonde. 2012. "Ultimate Shear Strength of Ultra High Performance Fibre-Reinforced Concrete Beams." In *Ultra-High-Performance Concrete and Nanotechnology in Construction: Proceedings of HiPerMat 2012. 3rd International Symposium on Ultra-High-Performance Concrete and Nanotechnology for High Performance Construction Materials Kassel, March 7-9, 2012*, edited by M. Schmidt, E. Fehling, C. Glotzbach, S. Fröhlich, and S. Piotrowski, 485–492. Kassel, Germany: Kassel University Press. https://www.uni-kassel.de/ub/publizieren/kassel-university-press/verlagsprogramm?h=9783862192649.

24. Mészöly, T., and N. Randl. 2018. "Shear Behavior of Fiber-Reinforced Ultra-High Performance Concrete Beams." *Engineering Structures*, no. 68: 119–127. https://

doi.org/10.1016/j.engstruct.2018.04.075.

25. Yap, B. 2020. "Behaviour of Ultra High Performance Fibre Reinforced Concrete Subjected to Pure Shear," PhD diss., University of Toronto. https://hdl.handle.net/1807/100927.

26. Voss, M. S., K. A. Riding, R. S. Alrashidi, C. C. Ferraro, and H. R. Hamilton. 2022. "Comparison between Direct Tension, Four-Point Flexure, and Simplified Double-Punch Tests for UHPC Tensile Behavior," *Journal of Materials in Civil Engineering* 34 (9). https://doi.org/10.1061/(ASCE)MT.1943-5533.0004371.

27. El-Helou, R. G., Z. B. Haber, and B. A. Graybeal. 2022. "Mechanical Behavior and Design Properties of Ultra-High-Performance Concrete." *Materials Journal* 119 (1): 181–194. https://doi.org/10.14359/51734194.

28. Wu, X., and S. M. Han. 2009. "First Diagonal Cracking and Ultimate Shear of I-Shaped Reinforced Girders of Ultra High Performance Fiber Reinforced Concrete without Stirrup." *International Journal of Concrete Structures and Materials* 3 (1): 47–56. https://doi.org/10.4334/IJCSM.2009.3.1.047.

29. Jabbar, A. M., M. J. Hamood, and D. H. Mohammed. 2021. "The Effect of Using Basalt Fibers Compared to Steel Fibers on the Shear Behavior of Ultra-High Performance Concrete T-Beam." *Case Studies in Construction Materials*, no. 15: e00702. https://doi.org/10.1016/j.cscm.2021.e00702.

30. Țibea, C., and D. V. Bompa, D. 2020. "Ultimate Shear Response of Ultra-High-Performance Steel Fibre-Reinforced Concrete Elements." *Archives of Civil and Mechanical Engineering*, no. 20: 49. https://doi.org/10.1007/s43452-020-00051-z.

31. Chen, B., J. Zhou, D. Zhang, K. Sennah, and C. Nuti. 2023. "Shear Performances of Reinforced Ultra-High Performance Concrete Short Beams." *Engineering Structures*, no. 277: 115407. https://doi.org/10.1016/j.engstruct.2022.115407.

32. Chen, B., J. Zhou, D. Zhang, J. Su, C. Nuti, and K. Sennah. 2022. "Experimental Study on Shear Performances of Ultra-High Performance Concrete Deep Beams." *Structures*, no. 39: 310–322. https://doi.org/10.1016/j.istruc.2022.03.019.

33. El-Helou, R. G., and B. A. Graybeal. 2022. "Shear Behavior of Ultrahigh-Performance Concrete Pretensioned Bridge Girders." *Journal of Structural Engineering* 148 (4). https://doi.org/10.1061/(ASCE)ST.1943-541X.0003279.

34. El-Helou, R. G., and B. A. Graybeal. 2023. "Shear Design of Strain-Hardening Fiber-Reinforced Concrete Beams." *Journal of Structural Engineering* 149 (2). https://doi.org/10.1061/JSENDH.STENG-11065.

35. Zeng, J. J., B. Z. Pan, T. H. Fan, and Y. Zhuge. 2023. "Shear Behavior of FRP-UHPC Tubular *Beams." Composite Structures* 307: 116576. https://doi.org/10.1016/j.compstruct.2022.116576.

36. Yang, J., J. H. Doh, K. Yan, and X. Zhang. 2022. "Experimental Investigation and Prediction of Shear Capacity for UHPC Beams." *Case Studies in Construction Materials*, no. 16: e01097. https://doi.org/10.1016/j.cscm.2022.e01097.

37. Chen, B. 2007. "Study on the Shear Strength of Prestressed RPC Girders." Master's thesis, Hunan University, Changsha, China.

38. Zhang, P. 2011. "Study on Oblique Section Shear-Bearing Capacity of RPC Beam Based on Softened Truss Theory." Master's thesis, Beijing Transportation University (CNKI Database).

39. Feng, W., H. Feng, Z. Zhou, and X. Shi. 2021. "Analysis of the Shear Capacity of Ultrahigh Performance Concrete Beams Based on the Modified Compression Field Theory." *Advances in Materials Science and Engineering*, no. 2021: 5569733. https://doi.org/10.1155/2021/5569733.

40. Vandewalle, L., D. Nemegeer, L. Balazs, B. Barr, J. Barros, P. Bartos, N. Banthia, M. Criswell, E. Denarie, M. Di Prisco, and H. Falkner. 2003. "RILEM TC 162-TDF: Test and Design Methods for Steel Fibre Reinforced Concrete'-Sigma-Epsilon-Design Method-Final Recommendation." *Materials and Structures* 36 (262): 560–567. https://doi.org/10.1617/14007.

41. AFNOR (Association Française de Normalisation). 2016. *National Addition to Eurocode 2—Design of Concrete Structures: Specific Rules for Ultra-High Performance Fiber-Reinforced Concrete (UHPFRC).* NF P18-710. Saint-Denis, France: AFNOR Editions.

42. SIA (Swiss Society of Engineers and Architects). 2014. *Béton Fibré Ultra-Performant (BFUP); Matériaux, Dimensionnement et Exécution* [Ultra-High-Performance Fiber-Reinforced Concrete (UHPC)—Materials, Sizing, and Execution]. SIA 2052. Zurich, Switzerland: SIA.

43. López, J. A., P. Serna, and J. Navarro-Gregori. 2017. "Advances in the Development of the First UHPFRC Recommendations in Spain: Material Classification, Design and Characterization." In *UHPFRC 2017 Designing and Building with UHPFRC: New Large-Scale Implementations, Recent Technical Advances, Experience and Standards*, edited by F. Toutlemonde and J. Resplendino,

565–574. Champs-sur-Marne, France: RILEM Publications SARL.

44. Schmidt, M., T. Leutbecher, S. Piotrowski, and U. Wiens. 2017. "The German Guideline for Ultra-High Performance Concrete." In *UHPFRC 2017 Designing and Building with UHPFRC: New Large-Scale Implementations, Recent Technical Advances, Experience and Standards*, edited by F. Toutlemonde and J. Resplendino, 545–554. Champs-sur-Marne, France: RILEM Publications SARL.

45. AASHTO (American Association of State Highway and Transportation Officials). 2024. *AASHTO LRFD Bridge Design Specifications*. Washington, DC: AASHTO.

46. Vecchio, F. J., and M. P. Collins. 1986. "The Modified Compression-Field Theory for Reinforced Concrete Elements Subjected to Shear." *ACI Journal Proceedings* 83 (2): 219–231. https://doi.org/10.14359/10416.

47. ASTM International. 2024. *Standard Test Method for Flexural Performance of Fiber-Reinforced Concrete (Using Beam with Third-Point Loading)*. ASTM C1609/C1609M-24. West Conshohocken, PA: ASTM International.

48. CSA Group. 2019. *Canadian Highway Bridge Design Code*. CSA S6:19. Toronto, ON: CSA Group.

49. Graybeal, B. A., and R. G. El-Helou. 2019. "Development of an AASHTO Guide Specification for UHPC." *International Interactive Symposium on Ultra-High Performance Concrete* 2 (1). https://doi.org/10.21838/uhpc.9708.

50. Vu, D. T., and N. D. Hoang. 2016. "Punching Shear Capacity Estimation of FRP-Reinforced Concrete Slabs Using a Hybrid Machine Learning Approach." *Structure and Infrastructure Engineering* 12 (9): 1153–1161. https://doi.org/10.1080/15732479.2015.1086386.

51. Yan, K., and C. Shi. 2010. "Prediction of Elastic Modulus of Normal and High Strength Concrete by Support Vector Machine." *Construction and Building Materials* 24 (8): 1479–1485. https://doi.org/10.1016/j.conbuildmat.2010.01.006.

52. Lee, S., and C. Lee. 2014. "Prediction of Shear Strength of FRP-Reinforced Concrete Flexural Members without Stirrups Using Artificial Neural Networks." *Engineering Structures*, no. 61: 99–112. https://doi.org/10.1016/j.engstruct.2014.01.001.

53. Diab, A., and A. Ferche. 2023. "Prediction of the Tensile Properties of UHPC Using Artificial Neural Network." *Structural Journal* 121 (2): 57–69. https://doi.org/0.14359/51740245.

54. Castelli, M., L. Vanneschi, and S. Silva. 2013. "Prediction of High Performance Concrete Strength Using Genetic Programming with Geometric Semantic Genetic Operators." *Expert Systems with Applications* 40 (17): 6856–6862. https://doi.org/10.1016/j.eswa.2013.06.037.

55. Kara, I. F. 2011. "Prediction of Shear Strength of FRP-Reinforced Concrete Beams without Stirrups Based on Genetic Programming." *Advances in Engineering Software* 42 (6): 295–304. https://doi.org/10.1016/j.advengsoft.2011.02.002.

56. Ahmad, S., S. Bahij, M. A. Al-Osta, S. K. Adekunle, and S. U. Al-Dulaijan. 2019. "Shear Behavior of Ultra-High-Performance Concrete Beams Reinforced with High-Strength Steel Bars." *Structural Journal* 116 (4): 3–14. https://doi.org/10.14359/51714484.

57. Solhmirzaei, R., H. Salehi, V. Kodur, and M. Z. Naser. 2020. "Machine Learning Framework for Predicting Failure Mode and Shear Capacity of Ultra High Performance Concrete Beams." *Engineering Structures*, no. 224: 111221. https://doi.org/10.1016/j.engstruct.2020.111221.

58. Zheng, H., Z. Fang, and B. Chen. 2019. "Experimental Study on Shear Behavior of Prestressed Reactive Powder Concrete I-Girders." *Frontiers of Structural and Civil Engineering* 13 (3): 618–627. https://doi.org/10.1007/s11709-018-0500-8.

59. Baby, F., J. Billo, J. C. Renaud, C. Massotte, P. Marchand, F. Toutlemonde, A. Simon, and P. Lussou. 2010. "Shear Resistance of Ultra High Performance Fibre-Reinforced Concrete I-Beams." In *Fracture Mechanics of Concrete and Concrete Structures: High Performance, Fiber Reinforced Concrete, Special Loadings and Structural Applications*, edited by B. H. Oh, O. C. Choi, and L. Chung. Seoul, Korea: Korea Concrete Institute. https://www.framcos.org/FraMCoS-7/12-05.pdf.

60. Yang, I. H., C. Joh, and B. S. Kim. 2012. "Shear Behaviour of Ultra-High-Performance Fibre-Reinforced Concrete Beams without Stirrups." *Magazine of Concrete Research* 64 (11): 979–993. https://doi.org/10.1680/macr.11.00153.

61. Jin, L. Z., X. Chen, F. Fu, X. F. Deng, and K. Qian. 2020. "Shear Strength of Fibre-Reinforced Reactive Powder Concrete I-Shaped Beam without Stirrups." *Magazine of Concrete Research* 72 (21): 1112–1124. https://doi.org/10.1680/jmacr.18.00525.

62. Baby, F., P. Marchand, and F. Toutlemonde. 2014. "Shear Behavior of Ultrahigh Performance Fiber-Reinforced Concrete Beams. I: Experimental Investigation." *Journal of Structural Engineering* 140 (5). https://doi.org/10.1061/(ASCE)ST.1943-541X.0000907.

63. Voo, J. Y. L., and S. J. Foster. 2003. "Variable Engagement Model for the Design of Fibre Reinforced Concrete Structures." In *Advanced Materials for Construction of Bridges, Buildings, and Other Structures III*, edited by V. Mistry, A. Azizinamini, and J. M. Hooks. New York: Engineering Conferences International. https://dc.engconfintl.org/advanced_materials/2.

64. Voo, Y. L., W. K. Poon, and S. J. Foster. 2010. "Shear Strength of Steel Fiber-Reinforced Ultrahigh-Performance Concrete Beams without Stirrups." *Journal of Structural Engineering* 136 (11): 1393–1400. https://doi.org/10.1061/(ASCE)ST.1943-541X.0000234.

65. Hegger, J., S. Rauscher, and C. Goralski. 2005. "Push-Out Tests on Headed Studs Embedded in UHPC." In *Seventh International Symposium on the Utilization of High Strength/High-Performance Concrete*. Farmington Hills, MI: American Concrete Institute. https://doi.org/10.14359/14503.

66. Graybeal, B. A. 2006. "Practical Means for Determination of the Tensile Behavior of Ultra-*High Performance Concrete*." *Journal* of ASTM International 3 (8): 1–9. https://doi.org/10.1520/JAI100387.

67. Chen, T., and C. Guestrin. 2016. "XGBoost: A Scalable Tree Boosting System," In *Proceedings of KDD '16: The 22nd ACM SIGKDD International Conference on Knowledge Discovery and Data Mining San Francisco California USA August 13–17, 2016*, 785–794. New York: Association for Computing Machinery. https://doi.org/10.1145/2939672.2939785.

Notation

a = shear span

A_c = area of the concrete cross section

A_{ct} = area of ultra-high-performance concrete on the flexural tension side of the member

A_i = actual measurements

A_{mean} = mean of the actual measurements

A_{ps} = area of prestressing steel on the flexural tension side of the member

A_s = areas area of non-prestressed steel on the flexural tension side of the member at the critical shear section

A_v = area of transverse reinforcement

b_v = effective web width taken as the minimum web width within the effective shear depth

b_w = web width

d = distance between the extreme compression fiber of the ultra-high-performance concrete section to the resultant of the forces in the tensile reinforcement

d_f = diameter of the fiber reinforcement

d_v = effective shear depth

E_c = Young's modulus of ultra-high-performance concrete

E_p = Young's modulus of the prestressing steel

E_s = Young's modulus of the reinforcing steel

f'_c = compressive strength of ultra-high-performance concrete

f_{po} = a parameter representing prestressing level taken as modulus of elasticity of prestressing steel multiplied by the locked-in difference in strain between the prestressing steel and the surrounding ultra-high-performance concrete

f_{rr} = residual tensile strength of the ultra-high-performance concrete material

$f_{t,loc}$ = crack localization strength

$f_{t,cr}$ = effective cracking strength

f_{vs} = yield stress of shear reinforcement

$f_{v,\alpha}$ = uniaxial stress in the transverse reinforcement

h = total height of the beam

$J(\theta)$ = objective function in machine learning

L_f = fiber reinforcement length

$L(\theta)$ = loss function in machine learning

M_u = factored moment at the critical shear section

n = number of predictions

N_u = factored axial force

P = prestressing force

P_e = prestressing force in the critical shear section

P_i = predictions

R^2 = coefficient of determination

s = spacing of transverse reinforcement, measured parallel to the longitudinal reinforcement

V_{exp} = experimental shear capacity results

V_f = fiber volume fraction

V_n = nominal shear resistance

$V_{n,eCPCI}$ = nominal shear resistance using eCPCI method

$V_{n,FHWA}$ = nominal shear resistance using Federal Highway Administration method

$V_{n,ML}$ = nominal shear resistance using machine learning

V_p = shear resistance provided by the vertical component of the effective prestressing force

V_{pred} = predicted shear capacity results

V_s = shear resistance provided by conventional transverse reinforcement

V_u = factored shear force at the critical shear section

V_{UHPC} = shear resistance provided by the ultra-high-performance concrete

y_i = actual result in machine learning

$\hat{y}_i$ = prediction result in machine learning

α = angle of inclination of the transverse reinforcement to the longitudinal axis

γ_u = shear capacity reduction factor to account for the variability in the tensile stress in ultra-high-performance concrete

ε_2 = strain in the compressive strut

ε_s = net longitudinal strain at the centroid of the tension reinforcement

$\varepsilon_{t,loc}$ = crack localization strain

ε_v = strain along the transverse direction

θ = angle of inclination of the diagonal compressive stress

λ = characteristic parameter of steel fiber

ρ_f = fiber reinforcement ratio

ρ_{ps} = prestressed steel reinforcement ratio

ρ_s = non-prestressed steel reinforcement ratio

ρ_t = tensile reinforcement ratio

ρ_v = shear reinforcement ratio

$\rho_{v,\alpha}$ = ratio of the cross-sectional area of the transverse steel reinforcement crossing the critical shear crack to the ultra-high-performance concrete gross area along the crack projected in the longitudinal direction

σ_p = prestressing level in the critical shear section

$\Omega(\theta)$ = regularization term in machine learning

About the authors

Brandon Ross, PhD, PE, is the Cottingham Professor in the Glenn Department of Civil Engineering at Clemson University in Clemson, S.C.

Ahmad Tarawneh, PhD, PE, is an associate professor in the Civil Engineering Department at the Hashemite University in Zarqa, Jordan.

M. Z. Naser, PhD, is an assistant professor in the Glenn Department of Civil Engineering at Clemson University.

Anca C. Ferche, PhD, is an assistant professor in the Department of Civil, Architectural, and Environmental Engineering at the University of Texas at Austin in Austin, Tex.

Amjad Y. Diab, MSc, is a PhD student in the Department of Civil, Architectural, and Environmental Engineering at the University of Texas at Austin.

Deanna Craig, MSc, graduated from the Glenn Department of Civil Engineering at Clemson University with a master's degree.

Abstract

This paper reports on an evaluation of two models for calculating the shear strength of prestressed ultra-high-performance concrete (UHPC) beams. Calculations from these models, referred to as the eCPCI and FHWA (Federal Highway Administration) models, were compared to a database of experimental test results compiled from the literature. Identifying comparable UHPC material properties from the published literature was a challenge because different testing programs used different material tests. Accordingly, UHPC localized tensile strength was estimated based on the available data and approximate ratios. In addition to the experimental database, a machine-learning prediction model was developed to generate a simulation database used for further evaluation of the eCPCI and FHWA models. On average, the FHWA model resulted in shear capacity estimates that were 17% lower than the eCPCI method. However, the analyses show that shear strength predictions from both the FHWA and eCPCI models were typically conservative relative to data from the experimental and simulated databases. In addition, both models were observed to produce less-accurate estimates for larger-sized specimens than for smaller specimens.

Keywords

Beam shear behavior, machine learning, prestressed concrete, shear database, shear design model, UHPC, ultra-high performance concrete.

Review policy

This paper was reviewed in accordance with the Precast/Prestressed Concrete Institute's peer-review process. The Precast/Prestressed Concrete Institute is not responsible for statements made by authors of papers in *PCI Journal*. No payment is offered.

Publishing details

This paper appears in *PCI Journal* (ISSN 0887-9672) V. 69, No. 6, November–December 2024, and can be found at https://doi.org/10.15554/pcij69.6-01. *PCI Journal* is published bimonthly by the Precast/Prestressed Concrete Institute, 8770 W. Bryn Mawr Ave., Suite 1150, Chicago, IL 60631.

Reader comments

Please address any reader comments to *PCI Journal* editor-in-chief Tom Klemens at tklemens@pci.org or Precast/Prestressed Concrete Institute, c/o *PCI Journal*, 8770 W. Bryn Mawr Ave., Suite 1150, Chicago, IL 60631.